Article

Stability of dielectric properties of aluminum under gamma-quantum irradiation

Adilzhan Omarov[1,*], Aigul Zhantasova[1], Almas Siddiqui[2]

[1]Faculty of Computer Science, Toraighyrov Pavlodar University, 64 Lomov st., Pavlodar, Kazakhstan
[2]Division of Physical and Mathematical Sciences, Indian Institute of Science Bangalore, 54 Raman Rd., Bengaluru, India
*Correspondence: omarov.adilzhan@list.ru

Abstract. In this work was to reveal the effects of gamma-quantum irradiation on the microstructure and electrophysical characteristics of aluminum. The effects of gamma irradiation with a radionuclide source of cesium-137 isotope on the properties of aluminum were studied. The maximum absorbed doses were approximately 10^8 rads. Aluminum plates with a thickness of 6 mm and an area of 5 cm^2 were utilized during the experiments. The main challenge in obtaining reliable, adequate automated adaptation of the gamma spectrometer under conditions of change in a certain range of characteristics of the water environment (such as, for example, temperature and pressure) is the task of obtaining reliable, high-quality and reliable measurements. The paper presents the results of testing and adjustment of the complex of autonomous automated calibration of ^{137}Cs gamma-spectrometer. The processes occurring during gamma-quantum irradiation of aluminum and their influence on dielectric properties of the material were studied. The results obtained indicate that when aluminum is irradiated with a dose of 10^8 rad, only a slight change in its dielectric permittivity is observed.
Keywords: gamma ray, irradiation, ^{137}Cs isotope, semiconductors, aluminum.

1. Introduction

It is known that irradiation of metals, semiconductor crystals and alloys with gamma quanta can lead to disruption of their structure by introducing radiation defects [1-3]. These defects can include point defects such as vacancies and interstitial atoms as well as linear defects such as dislocations. Radiation defects can affect the mechanical, electrical, and magnetic properties of materials, making gamma ray irradiation an important factor in studying the behavior of materials under radiation exposure.

However, in the study [4-5] it was found that the irradiation of metals, semiconductors and alloys by gamma-quanta with an exposure dose of more than 10^5 J/kg does not lead to the accumulation of defects, but, on the contrary, promotes their elimination and leads to the transition of the material to a more stable state compared to its initial state. An interesting phenomenon is that such effects of ionizing radiation cause rearrangement of the metal structure and consequently lead to changes in its electrophysical properties.

In the modern electrical industry, considerable importance is attached to the use of aluminum and its oxides because of their semiconducting properties [6-7]. These materials offer a number of advantages such as high thermal conductivity, strength and low density, making them an ideal choice for many applications in electronics and electrical engineering. Their use enables the creation of components with high efficiency and reliability, which is important for modern technology and industrial processes.

Other scientists have studied the effect of ionizing radiation on the stability of semiconductor devices [8-9]. Moreover, gamma radiation has a particularly negative impact, as it has a high

penetrating ability and is characterized by the lack of effective protection methods. This property of gamma radiation makes it especially dangerous for semiconductor devices, as it is able to penetrate through ordinary materials and cause significant changes in their structure and functionality. As a result, the development of methods of protection against gamma radiation and the study of its effects on semiconductor devices are important areas of research in the field of electronics and electrical engineering [10]. Therefore, the main aspect of our study is to investigate the effect of gamma rays on the characteristics of aluminum.

The primary challenge in achieving accurate and high-quality measurements lies in implementing an effective automated adaptation mechanism for the gamma-spectrometer, particularly when faced with variations in key environmental parameters within the water medium, such as temperature and pressure. This paper outlines the outcomes of testing and fine-tuning procedures conducted on the autonomous automated calibration system for Cs137 gamma-spectrometers.

2. Methods

In this work, optical and mechanical experimental methods were used to study radiation damage in the structure of an irradiated aluminum plate sample, both in the volume and in the surface layer with gamma radiation sources of radioactive isotopes Cs^{137} of 662 keV. The number of radiation sources, their location and the configuration of the chamber guaranteed a uniform gamma ray flux. The irradiation was performed in a closed chamber containing oxygen at normal room temperature. The irradiation rate was constant at 65 rad/s, and the maximum absorbed doses were $\sim 10^8$ rads. Aluminum plates were used with a thickness of 6 mm, area 5 cm^2.

A gamma radiation source of the Cs^{137} crystals were used as ionizing radiation, the flashes of which were recorded using light-sensitive devices as a photomultiplier tube (PMT) based on NaI (Tl) crystal.

The NaI (Tl) scintillation detector coupled with a PMT operates as a highly efficient system for detecting and measuring gamma rays and other forms of ionizing radiation. The core component, the NaI (Tl) crystal, is a thallium-doped sodium iodide scintillator, which plays a crucial role in the detection process [11].

Figure 1 presents a block diagram illustrating the configuration of the spectrometer system.
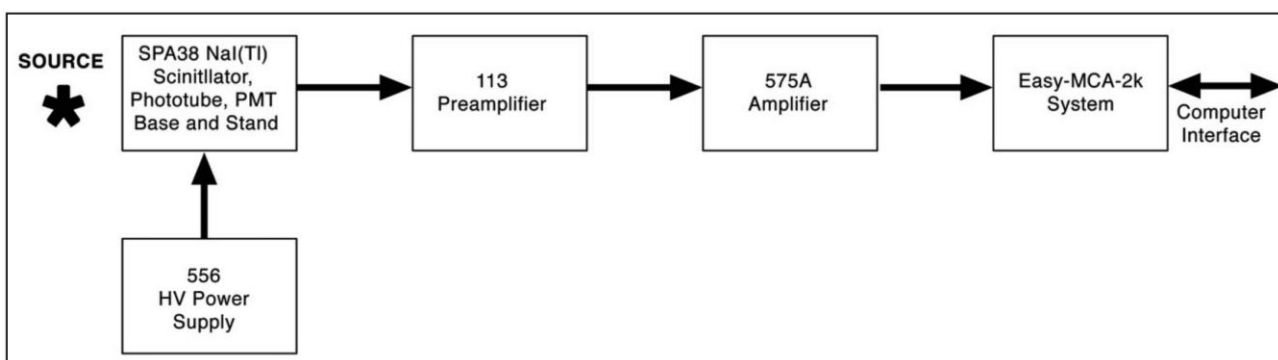

Figure 1 − Block diagram showcasing the electronics setup for a gamma-ray spectroscopy system employing a NaI (Tl) detector [12]

Initially, the preamplifier gathers the charge accumulated on the anode via a capacitor, converting this charge into a voltage pulse. This pulse is then relayed to the subsequent amplifier for further processing. The magnitude of the voltage pulse at both the output of the preamplifier and the output of the linear amplifier is directly proportional to the energy imparted to the scintillator by the gamma ray being detected [12].

The Universal Computer Spectrometer (UCS) system is specifically engineered to interface seamlessly with personal computers via a USB connection. To ensure both stable performance and

minimal noise interference, the device utilizes an alternating current (AC) power source, accommodating a wide voltage range from 100 to 250 V AC through an automatically adjusting power supply. The device incorporates a microprocessor that functions as the central processing unit and data storage medium, facilitating direct communication with the PC through the USB interface.

As a calibration sample was used Cs^{137} isotopes of round shape, 2.5 cm in diameter, which were placed on a tray located on the secondary rack. The parameters of gamma irradiation were set as follows: voltage 450 V, number of channels – 1024, fine grain – 1.0, course gain – 16, lower discriminator – 0, upper discriminator - 1024. After an interval of 500 seconds, spectral data were acquired. Reference values corresponding to characteristic isotope peaks were used to ensure the accuracy of the energy calibration. Control of calibration accuracy consists in calculation of backscattering peaks and Compton edge.

After this calibration, the accuracy of registration is checked by calculation of backscatter peaks and Compton edge. At this stage, the Cs^{137} sample is moved to the third rack of the experimental setup and then an aluminum plate is installed.

Optical absorption spectra were measured on a Phywe spectrometer corrected for the thickness of each sample. The mass absorption coefficient of the aluminum plate sample was determined, which is found using Lambert's Law about the decrease of intensity of radiation [13]:

$$I = I_0 e^{-\mu x} \qquad (1)$$

Where: I – intensity after the absorber; I_0 – intensity before the absorber; μ – total-mass absorption coefficient, cm^2/g ; x - density thickness g/cm^2.

To determine the absorption coefficient, the natural logarithm of the ratio $\ln \frac{I}{I_0} = -\mu x$ was plotted and fitted to a linear regression line, where $\frac{N}{N_0} = \frac{I}{I_0}$ represents the net number of counts obtained in each measurement with the aluminum plate placed between the source and detector, and N_0 denotes the number of counts obtained without attenuation. The intensity I is proportional to the number of samples, so $\frac{N}{N_0}$ corresponds to the ratio of intensities $\frac{I}{I_0}$.

To quantify the number of samples, a region of interest (ROI) around the 662 keV peak is defined. By selecting this region of interest in the program spectrum, the number of clean counts in this region as well as the full width half-maximum (FWHM) of the peak can be obtained. Then, by measuring the decrease in the number of clean counts in the 662 keV peak for each additional aluminum plate introduced between the source and detector, the absorption coefficient is calculated.

For an extended view, we considered the effect of gamma radiations on the dielectric properties of aluminum.

3. Results and Discussion

Due to their high penetrating ability, gamma quanta can affect the electrophysical characteristics of metals, semiconductors and metals [14-16].

Figure 2 depicts the dual peaks resulting from a Cs^{137} radioisotope. The energy spectrum of cesium-137 was calibrated at 450 V and gain 16 sec. The scan area covered energies from 590 keV to 706 keV. The clean counts are displayed in the lower right corner of the software interface, thus no aluminum plates were installed between the source and detector. The decay process primarily involves a beta emission, with over 93% of occurrences, leading to the 661.6 keV excited state of Cs^{137}.

Subsequently, decay to the ground state follows through a 661.6 keV gamma-ray emission. Additionally, there is consistently a noticeable peak of X-ray radiation at 32 keV [16-18], which serves as a calibration reference. Therefore, the main energy channel in cesium is at an energy of 662 keV, and Compton scattering is observed at an energy of 30 keV.

Two characteristic peaks are observed on the energy spectrum: the Compton edge peak and the backscattering peak, labeled with energies of 208.72 keV and 463 keV, respectively.
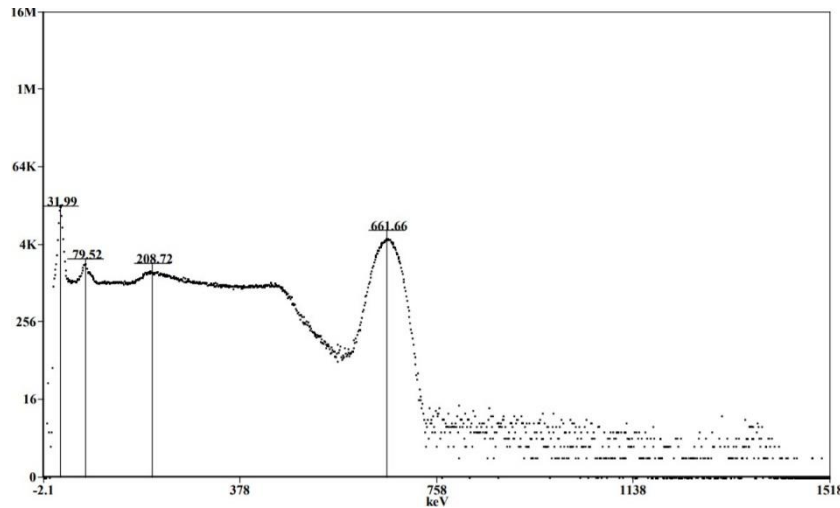
Figure 2 – Calibrated energy spectrum of Cs^{137} at 450 V

The first of them is caused by Compton scattering of gamma-quanta on the detector electrons, and its energy is calculated according to the Compton equation at Θ = 0 using the known value of the electron rest mass mc^2 = 511 keV. Accordingly, the energy of the Compton edge peak is 208.72 keV. The backscattering peak manifests itself as a result of backscattering of gamma quanta on the source electrons. Its energy corresponds to the energy of gamma quanta scattered by 180 degrees. Thus, the energy of the backscattering peak is 463 keV.

For a more accurate calculation of the photon energy after scattering of the irradiated sample of cesium isotope, we used the following formula:

$$E' = \frac{E}{1 + \frac{E}{mc^2}(1 - \cos\theta)} \qquad (2)$$

Where: E' – the energy of the scattered photon, keV; E – peak energy, keV; m – the mass of the electron, kg; c – the speed of light, m/s; θ – the angle of scattering of the gamma-ray, deg.

Figure 3 shows the gamma ray spectra of aluminum plate, which was placed between the radiation source and the detector during the measurements.
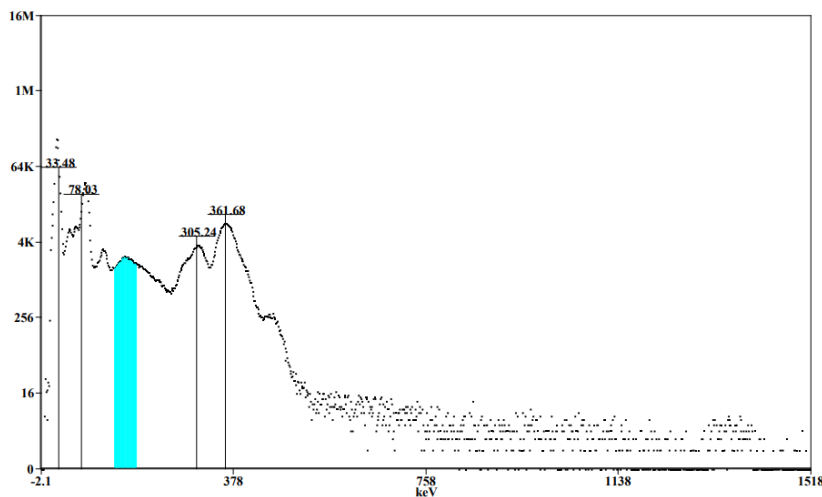

Figure 3 – A calibrated energy spectrum of ^{137}Cs acquired at a voltage of 450V and with a coarse gain setting of 16

A ROI has been defined spanning from 590 keV to 706 keV. The net counts corresponding to this ROI are displayed in the bottom right corner of the software interface. An aluminum plate was positioned between the radiation source and the detector during the measurements.

Given the premise that the energy of the scattered photon equals the sum of the energies of the scattered electron and the incident wave, we can derive the energy of the scattered electron as

follows: $E'_e = E' = E$, where, E'_e – the energy of the scattered electron, keV; E' – the energy of the scattered photon, keV; E - peak energy, keV.

The calculated value of the backscattering peak energy for ^{137}Cs is 184.32 keV and the maximum Compton edge energy is 477.34 keV. This close agreement with theoretical expectations indicates a well-calibrated system, as it reflects the expected energy level for backscattered photons in this experimental setup [17-19].

According to the data obtained in Table 1, the number of gamma photons that deviate from the photopeak due to photoelectric or Compton interactions occurring in the aluminum absorber placed between the radiation source and the detector was detected.

Table 1 – The mass absorption coefficient of the Aluminium for E=662 keV

The theoretical mass absorption coefficient, cm^2/g	Experimental obtained mass absorption coefficient, cm^2/g
0.078	0.063±0.007

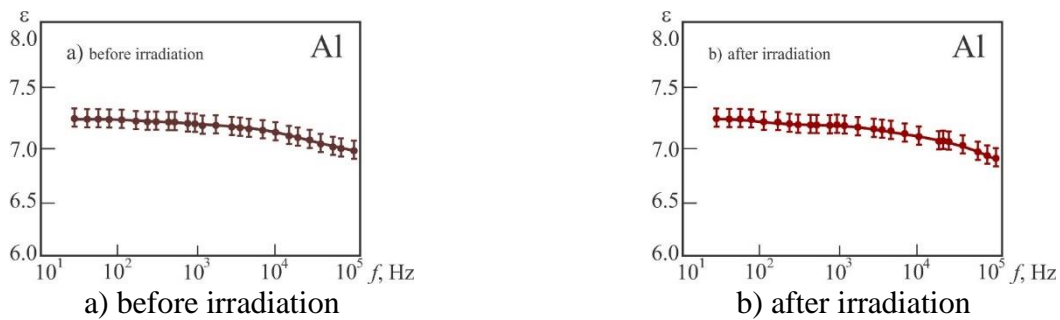a) before irradiation   b) after irradiation

Figure 4 – The dependence of frequency on dielectric permittivity

Figure above shows the dependence of frequency on dielectric permittivity before (Figure 4a) and after (Figure 4b) irradiation. In the observed frequency range, an increase in frequency was accompanied by a slight decrease in the value of e. It was found that after irradiation of aluminum samples with ^{137}Cs radionuclides to a dose of 10^8 rad, the dielectric constant remained almost unchanged over the entire frequency range, as shown in Figure 4b.

Due to the fact that aluminum is characterized by a forbidden zone width E_g from 5.1 to 8.8 eV, under normal conditions the concentration of electrons in the conduction band remains low, which entails negligible conductivity of this material.

4. Conclusions

In this work, the effect of gamma radiation ^{137}Cs isotope source irradiation on the properties of aluminum was presented, detailed calibration of the spectrophotometer was performed by decomposition of energy spectra, determination of the mass absorption coefficient of aluminum, and the dependence of the dielectric constant of aluminum on gamma radiation was shown.

As a result of the study, it was found that irradiation of aluminum samples with ^{137}Cs radionuclides up to a dose of 10^8 rad has no significant effect on the dielectric constant of this material in a wide frequency range. The observed insignificant change in the electrical properties of aluminum after irradiation can be explained by its peculiarities, such as the width of the forbidden zone. Thus, the results of the study confirm the stability of dielectric properties of aluminum under irradiation with ^{137}Cs radionuclides up to the considered irradiation dose.

References

1. Defects and radiation damage in metals / M.W. Thompson. — Cambridge, UK: University press, 1969. — 394 p.
2. Point Defects in Solids / A. Holland. — New York, USA: Springer, 1972. — 556 p.
3. Dynamics of annihilation of defects in semiconductor crystals under the action of small radiation doses / P.A. Cherdantsev, I.P. Chernov, Yu.A. Timoshnikov, V.A. Korotchenko, A.P. Mamontov // Soviet physics. Semiconductors. — 1984. — Vol. 18, No. 11. — P. 1283–1285.

4. Chain annihilation of defects in semiconductor crystals / P.A. Cherdantsev, I.P. Chernov, A.P. Mamontov // Soviet physics. Semiconductors. — 1982. — Vol. 16, No. 3. — P. 305–308.
5. Mechanism of radiation ordering of semiconductor crystals by means of low doses of irradiation / P.A. Cherdantsev, I.P. Chernov, A.P. Mamontov // Radiation effects. — 1982. — Vol. 60, No. 1–4. — P. 67–71. https://doi.org/10.1080/00337578208242777
6. High-κ gate dielectrics: Current status and materials properties considerations / G.D. Wilk, R.M. Wallace, J.M. Anthony // J. Appl. Phys. — 2001. — Vol. 89. — P. 5243–5275. https://doi.org/10.1063/1.1361065
7. Atomic layer deposition of titanium dioxide films using a metal organic precursor (C12H23N3Ti) and H2O (DI water) / B. Kim, N. Lee, S. Park, T. Park, J. Song, S. Han, H. Park, D. Lee, H. Kim, H. Jeon // Journal of Alloys and Compounds. — 2021. — Vol. 857. — P. 157931. https://doi.org/10.1016/j.jallcom.2020.157931
8. Particle interaction and displacement damage in silicon devices operated in radiation environments / C. Leroy, P.G. Rancoita // Reports on Progress in Physics. — 2007. — Vol. 70. No. 4. — P. 493. https://doi.org/10.1088/00344885/70/4/R01
9. Effects of γ-radiation on dielectric properties of LDPE–Al2O3 nanocomposites / F. Ciuprina, T. Zaharescu, I. Pleşa // Radiation Physics and Chemistry. — 2013. — Vol. 84. — P. 145–150. https://doi.org/10.1016/j.radphyschem.2012.06.028
10. Total ionizing dose effects in MOS oxides and devices / T.R. Oldham, F.B. McLean // IEEE Transactions on Nuclear Science. — 2003. — Vol. 50. No. 3. — P. 483–499. https://doi.org/10.1109/TNS.2003.812927
11. The photo-multiplier radiation detector / Marshall, Fitz-Hugh, J. W. Coltman, A. I. Bennett // Review of Scientific Instruments. — 1948. — Vol. 19. No. 11. — P. 744–770. http://doi.org/10.1063/1.1741156
12. Gamma-Ray Spectroscopy Using NaI(Tl) [Electronic resource]. — [2017]. — Mode of access: https://www.ortec-online.com/-/media/ametekortec/third%20edition%20experiments/3-gamma-ray-spectroscopy-using-nai-tl.pdf (accessed date: 18.07.2023).
13. The distribution in direction of photoelectrons from alkali metal surfaces / I.E. Herbert, A.R. Olpin, A.L. Johnsrud // Physical Review. — 1928. — Vol. 32. No. 1. — P. 57–80. https://doi.org/10.1103/PhysRev.32.57
14. The dielectric properties and radiation resistance of aluminum oxide layers obtained by atomic layer deposition / D. Dolzhenko, V. Kapralova, N. Sudar // Proceedings of the 2018 IEEE International Conference on Electrical Engineering and Photonics. — 2018. — P. 8564381. https://doi.org/10.1109/EExPolytech.2018.8564381
15. Neutron and Gamma Irradiation Effects on Power Semiconductor Switches / G. E. Schwarze, A. J. Frasca // Nasa Technical Memorandum. — 1990. — Vol. 1. — P. 103200.
16. Metal and Alloy Bonding - An Experimental Analysis / M. Prema Rani, R. Saravanan. — New York, USA: Springer, 2012. — 151 p.
17. Health Physics and Radiological Health, 4th Edition. / D. Pfeiffer // Medical Physics. — 2013. — Vol. 40, No. 11. — P. 117301. https://doi.org/10.1118/1.4826186
18. NNDC | National Nuclear Data Center [Electronic resource]. — [2023]. — Mode of access: https://www.nndc.bnl.gov/ (accessed date: 18.07.2023).
19. Table of Radioactive Isotopes Database [Electronic resource]. — [2023]. — Mode of access: https://application.wiley-vch.de/books/info/0-471-35633-6/toi99/www/decay/tori.htm (accessed date: 18.07.2023).

Information about authors:
Adilzhan Omarov – Master Student, Faculty of Computer Science, Toraighyrov Pavlodar University, 64 Lomov st., Pavlodar, Kazakhstan, omarov.adilzhan@list.ru
Aigul Zhantasova – Master Student, Faculty of Computer Science, Toraighyrov Pavlodar University, 64 Lomov st., Pavlodar, Kazakhstan, zhantasova.aigul@mail.ru
Almas Siddiqui – PhD Student, Division of Physical and Mathematical Sciences, Indian Institute of Science Bangalore, 54 Raman Rd., Bengaluru, India, almsiddiqui@gmail.com

Author Contributions:
Adilzhan Omarov – concept, methodology, funding acquisition, testing.
Aigul Zhantasova – interpretation, editing, modeling, resources.
Almas Siddiqui – visualization, analysis, data collection, drafting.